

# Accurate Solution of Square Scatterer as Benchmark for Validation of Electromagnetic Modeling of Plate Structures

Branko M. Kolundžija, *Member, IEEE*

**Abstract**—An infinitesimally thin-square scatterer, of size  $\lambda \times \lambda$ , excited normally by an incident plane wave, which is polarized along a scatterer edge, is analyzed. The accurate solution of its current distribution is found in the form of double series of basis functions, which automatically satisfy the continuity equation at plate edges and include the edge effect. The coefficients that multiply basis functions are determined starting from the electric field integral equation by using the Galerkin method. The solution obtained for the order of approximation  $n = 8$  is adopted as a benchmark. The corresponding coefficients are tabulated and graphs of such obtained current distribution are given. The solution adopted as a benchmark is applied for comparison of rooftop basis functions and polynomial entire-domain basis functions. The relative error of the mean absolute value of current deviation is used as an error metric.

**Index Terms**—Electromagnetic scattering, moment methods.

## I. INTRODUCTION

THEORETICALLY speaking, any plate structure (metallic antenna, scatterer, or passive circuit) in vacuum can be analyzed by the method of moments [1]. The efficiency of the analysis depends very much on the complexity of the structure on the one side and on the choice of the integral equation, basis functions and test procedure on the other side. Depending on these choices, many different specific methods have been developed in the last three decades [2]–[14].

Most often, the accuracy of these methods is subjectively discussed by comparing the theoretical and the experimental results. In order to treat the error quantitatively two things are needed: 1) an accurate benchmark to which we may apply the metric and 2) a metric to measure the error. To the best knowledge of the author, such quantitative treatment of the error in electromagnetic modeling of plates was absent.

In this paper, current distribution over an infinitesimally thin-square scatterer of size  $\lambda \times \lambda$  is chosen as a benchmark. The scatterer is excited normally by an incident plane wave, which is polarized along a scatterer edge. The relative error of the mean absolute value of current deviation is chosen as an error metric. These choices are explained in the second section.

The main problem in the paper is to find sufficiently accurate solution for current distribution over the scatterer. Each current component is approximated by double series

of basis functions multiplied by unknown coefficients. Basis functions are adopted in the special form, which automatically satisfies the continuity equation at plate edges and includes the edge effect. The development of basis functions applied is presented in the third section. Unknown coefficients are determined by the Galerkin method. The solution adopted as a benchmark (coefficients determined and such obtained current distribution) is given in the fourth section.

The solution adopted as a benchmark is used for comparing rooftop basis functions and polynomial entire-domain basis functions, as shown in the fifth section.

## II. CHOICE OF PLATE-STRUCTURE BENCHMARK AND ERROR METRIC

The main goal of electromagnetic modeling of plate structures based on the method of moments is to determine the current distribution. When the current distribution is known, all other quantities of interest can be easily calculated. Therefore, the error metric should be directly connected with the current distribution.

Most often, structures analyzed contain edges. Current distribution exhibits quasi-singular behavior in the vicinity of edges. Such behavior is more pronounced in the vicinity of a free plate edge than in the vicinity of an edge which is common for two or more plates. Hence, the structure used for comparison of analysis methods should contain free edges. The simplest such structure is a square-plate scatterer. The scatterer should be sufficiently large in order that accuracy of the analysis can be investigated in the large range of the number of unknowns. Hence, the structure used for the comparison of analysis methods is adopted in the form of infinitesimally thin-square scatterer of size  $\lambda \times \lambda$ , excited by normally incident plane wave. The effective value of plane wave electric field intensity is  $E = 1 \text{ V/m}$ .

At the first glance, it seems that the accuracy of the solution for current distribution of square-plate scatterer can be estimated on the base of root mean square (rms) value of the current deviation. The corresponding relative error is evaluated as

$$E_{\text{RMS}}[\%] = 100 \frac{\sqrt{\int_S |\mathbf{J}_s - \mathbf{J}_{s0}|^2 dS}}{\sqrt{\int_S |\mathbf{J}_{s0}|^2 dS}} \quad (1)$$

Manuscript received November 16, 1995; revised September 15, 1997.  
The author is with the Department of Electrical Engineering, University of Belgrade, Belgrade, 11120 Yugoslavia.  
Publisher Item Identifier S 0018-926X(98)05777-9.

where  $\mathbf{J}_s$  is an approximate,  $\mathbf{J}_{s0}$  is an accurate value of surface current density vector over the scatterer, and  $S$  is the scatterer

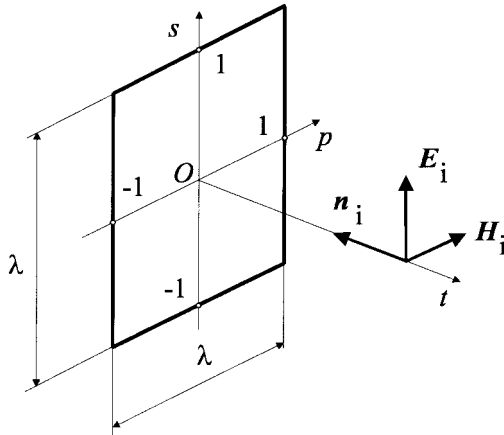


Fig. 1. Sketch of a square scatterer.

surface. However, this error metric cannot be used. Namely, it is known that the surface current component parallel to the free plate edge tends to infinity as a reciprocal value of the square root of the distance from the edge [15, p. 386]. It means that  $|\mathbf{J}_{s0}|^2$  tends to infinity as a reciprocal value of the distance from the edge. The integral of this function over the surface, i.e., the denominator in the above expression, is infinitely large. In a similar way it is found that the numerator in the above expression is also infinitely large. The finite value of the numerator and the denominator can be obtained if mean absolute value of current deviation is used instead of its rms value. The corresponding relative error is evaluated as

$$E[\%] = 100 \frac{\int_S |\mathbf{J}_s - \mathbf{J}_{s0}| dS}{\int_S |\mathbf{J}_{s0}| dS}. \quad (2)$$

This expression can be applied either to the total current or to the current components.

The use of the above error metric requires a knowledge of the accurate solution. However, there is no exact solution for current distribution over the square-plate scatterer. Hence, only the approximate solution, which is estimated to be sufficiently close to the accurate solution, can be used as an accurate solution. In this paper, such a solution is obtained by using sophisticated basis functions, as shown in the following section.

### III. ACCURATE SOLUTION OF SQUARE SCATTERER

Let us consider an infinitesimally thin-square-plate scatterer in a vacuum, as shown in Fig. 1. The scatterer is situated in a local  $ps$  coordinate system. Note that plate edges coincide with coordinate lines  $p = \pm 1$  and  $s = \pm 1$ . The scatterer is excited by a uniform plane wave incident normally on the scatterer surface. The wave is polarized in the direction of the  $s$  axis, i.e., the electric field vector  $\mathbf{E}_i$  is in the direction of the  $s$  axis and the magnetic field vector  $\mathbf{H}_i$  is in the direction of the  $p$  axis. As a result, surface currents (and charges) are induced over the scatterer.

Surface current density vector  $\mathbf{J}_s$  has two components, each of them depending on two surface coordinates; that is

$$\mathbf{J}_s(p, s) = J_{sp}(p, s)\mathbf{i}_p + J_{ss}(p, s)\mathbf{i}_s. \quad (3)$$

Note that  $p$ -current component is equal to zero at edges  $p = \pm 1$  and  $s$ -current component is equal to zero at edges  $s = \pm 1$ ; that is

$$J_{sp}(\pm 1, s) = 0, \quad J_{ss}(p, \pm 1) = 0. \quad (4)$$

Having in mind the symmetry of the problem considered it is easily concluded that  $p$ -current component is an odd function according to the local  $p$  and  $s$ -coordinate axis; that is

$$J_{sp}(p, s) = -J_{sp}(-p, s), \quad J_{sp}(p, s) = -J_{sp}(p, -s). \quad (5)$$

Similarly, it is concluded that  $s$ -current component is an even function according to the local  $p$  and  $s$ -coordinate axis; that is

$$J_{ss}(p, s) = J_{ss}(-p, s), \quad J_{ss}(p, s) = J_{ss}(p, -s). \quad (6)$$

As mentioned in the previous section, there is no exact solution for current distribution over the scatterer. The approximate solution is found by using the method of moments. According to this method each current component is approximated by a double series of known basis functions multiplied by unknown coefficients which should be determined. Very often, these basis functions are adopted in the form of subdomain basis functions (e.g., rooftop basis functions [7], triangle doublets [9], etc.). However, entire-domain basis functions enable more efficient analysis than subdomain basis functions [11]–[14]. Hence, the starting current distribution is adopted in the form of double series of power functions

$$J_{sp}(p, s) \cong \sum_{i=0}^{n_{sp}} \sum_{j=0}^{n_{pp}} a_{pij} s^i p^j, \quad J_{ss}(p, s) \cong \sum_{i=0}^{n_{ps}} \sum_{j=0}^{n_{ss}} a_{sij} p^i s^j \quad (7)$$

where  $a_{pij}$  and  $a_{sij}$  are unknown coefficients. Note that these expansions do not satisfy either continuity equations (4) or symmetry equations (5) and (6). Symmetry equations are easily satisfied by omitting terms not satisfying the symmetry equations from the above expansions. Continuity equations (4) can be implemented into above expansions by applying the technique given in [11] and [13]. After simple manipulations above, expansions are written in the form

$$J_{sp}(p, s) \cong \sum_{\substack{i=1 \\ (2)}}^{n_{sp}} \left\{ \sum_{\substack{j=3 \\ (2)}}^{n_{pp}} a_{pij} (p^j - p) \right\} s^i \quad (8)$$

$$J_{ss}(p, s) \cong \sum_{\substack{i=0 \\ (2)}}^{n_{ps}} \left\{ \sum_{\substack{j=2 \\ (2)}}^{n_{ss}} a_{sij} (s^j - 1) \right\} p^i. \quad (9)$$

Symbol (2) below the summation signs means that sums should be taken with a step of two.

Expansions (8) and (9) are very simple and flexible, but they cannot approximate edge effect properly. As mentioned in the previous section, the surface current component parallel to the free plate edge tends to the infinity as a reciprocal value of the square root of the distance from the edge. In order that such a behavior can be handled (8) is divided by  $\sqrt{1 - s^2}$  and (9) is divided by  $\sqrt{1 - p^2}$ . (Note that such edge condition

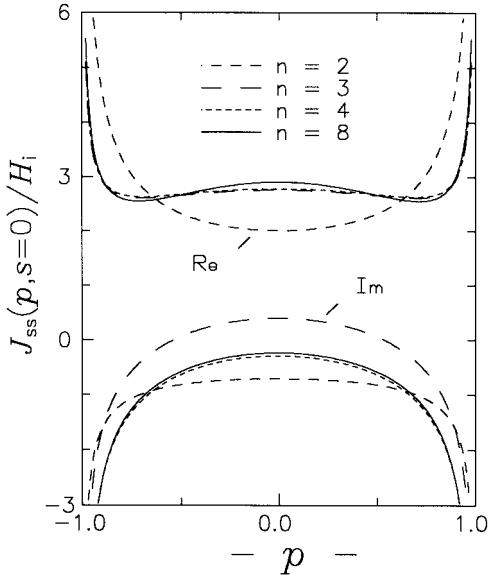


Fig. 2. Benchmark solution for the  $s$ -current component along the  $p$  axis of the scatterer (real and imaginary parts) obtained for different orders of current approximation.

is successfully applied in the analysis of two-dimensional problems, e.g., [16].) Final expansions are written in the form

$$J_{sp}(p, s) \cong \sum_{\substack{i=1 \\ (2)}}^{n_{sp}} \left\{ \sum_{\substack{j=3 \\ (2)}}^{n_{pp}} a_{pij}(p^j - p) \right\} \frac{s^i}{\sqrt{1-s^2}} \quad (10)$$

$$J_{ss}(p, s) \cong \sum_{\substack{i=0 \\ (2)}}^{n_{ps}} \left\{ \sum_{\substack{j=2 \\ (2)}}^{n_{ss}} a_{sij}(s^j - 1) \right\} \frac{p^i}{\sqrt{1-p^2}}. \quad (11)$$

Unknown coefficients in the above expansions are determined by using the Galerkin method. Special care is devoted to the evaluation of potential, field, and impedance integrals occurring in application of the Galerkin method.

#### IV. BENCHMARK SOLUTION: COEFFICIENTS AND GRAPHS

It is obvious that the approximate solution for current distribution over square scatterer depends on the choice of orders of current approximations along each coordinate  $n_{pp}$ ,  $n_{sp}$ ,  $n_{ps}$ , and  $n_{ss}$ . Having in mind that the scatterer length along the  $p$ -coordinate line is equal to the scatterer length along the  $s$ -coordinate line, all these orders can be adopted to be equal, i.e.,  $n_{pp} = n_{ps} = n_{ss} = n_{sp} = n$ . It can be shown that similar results are obtained if transverse orders are adopted to be less by one than longitudinal orders, i.e.,

$$n_{pp} = n_{ss} = n, \quad n_{ps} = n_{sp} = n - 1. \quad (12)$$

Such a choice is used in this paper. In what follows,  $n$  will be referred to as the order of the current approximation. Numerical results given in this and following section show that such choice enable good convergence of the results with increasing the order of current approximation  $n$ .

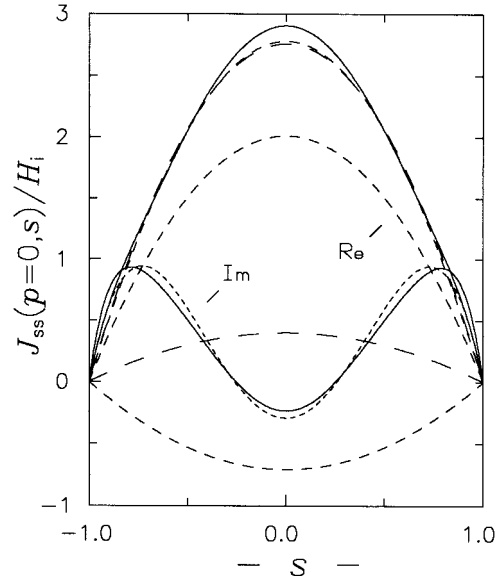


Fig. 3. Benchmark solution for the  $s$ -current component along the  $s$  axis of the scatterer (real and imaginary parts) obtained for different orders of current approximation.

TABLE I  
COEFFICIENTS OF  $p$ -CURRENT COMPONENT GIVEN BY (10) FOR  $n = 8$

$a_{pij} \cdot 10^3$	$j = 3$	$j = 5$	$j = 7$
$i = 1$	$0.412 + j 2.259$	$-0.365 - j 2.666$	$0.372 + j 1.657$
$i = 3$	$0.172 - j 1.931$	$-1.818 + j 4.995$	$0.911 - j 3.624$
$i = 5$	$-2.804 + j 2.101$	$6.718 - j 6.730$	$-3.823 + j 4.860$
$i = 7$	$2.217 - j 0.859$	$-5.085 + j 3.261$	$2.955 - j 2.391$

Let us consider how the approximate solution changes with increasing the order of current approximation  $n$ . Fig. 2 shows the real and the imaginary parts of the  $s$ -current component along  $p$ -coordinate line. The current is normalized with magnetic field intensity of incident plane wave. The results are given for  $n = 2, 3, 4$ , and  $8$ . Fig. 3 shows the same results, but along the  $s$ -coordinate line. The fast convergence of the results with increasing the order of approximation  $n$  can be observed from the figure. Further, it is seen that the results obtained for  $n = 4$  are very close to those obtained for  $n = 8$ . The results obtained for  $n = 5, 6$ , and  $7$  are between the results obtained for  $n = 4$  and  $8$ . The results obtained for  $n = 6, 7$ , and  $9$  coincide almost with the results obtained for  $n = 8$ . Hence, the results obtained for  $n = 5, 6, 7$ , and  $9$  are not shown in the figure.

The question is, "Which order of current approximation should be chosen for the benchmark solution?" On the one hand, the benchmark solution should be much more accurate than the solutions obtained by standard methods. On the other hand, the number of coefficients used in expansions (10) and (11) should be as low as possible so that the benchmark solution can be easily evaluated. According to these requests, order of current approximation  $n = 8$  is adopted for benchmark solution. Tables I and II provide corresponding coefficients of  $p$ -current component [given by (10)] and  $s$ -current component [given by (11)], all multiplied by  $10^3$ .

Figs. 4 and 5 show distribution of the magnitude, real part, and imaginary part of  $p$  and  $s$ -current components (normalized

TABLE II  
COEFFICIENTS OF  $s$ -CURRENT COMPONENT GIVEN BY (11) FOR  $n = 8$

$a_{sij} \cdot 10^3$	$j = 2$	$j = 4$	$j = 6$	$j = 8$
$i = 0$	$-9.622 + j 10.649$	$1.149 - j 14.536$	$6.534 + j 15.652$	$-5.763 - j 11.140$
$i = 2$	$7.492 - j 0.105$	$0.021 + j 5.201$	$-6.415 - j 9.338$	$5.686 + j 7.146$
$i = 4$	$-2.398 - j 1.720$	$1.509 - j 0.547$	$-0.545 + j 2.875$	$-0.502 - j 1.075$
$i = 6$	$0.265 + j 1.055$	$-1.003 + j 1.728$	$1.062 - j 5.947$	$-0.261 + j 3.714$

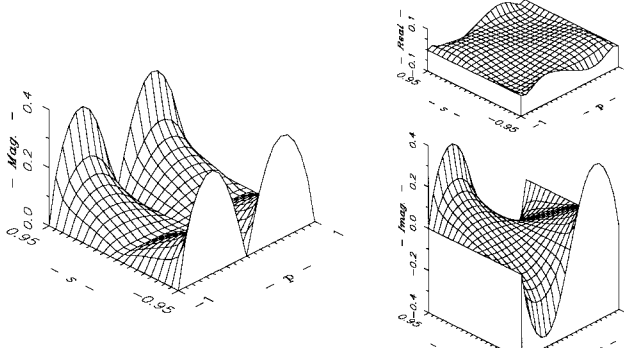


Fig. 4. Benchmark solution ( $n = 8$ ) for the  $p$ -current component over the scatterer. (a) Magnitude. (b) Real part. (c) Imaginary part.

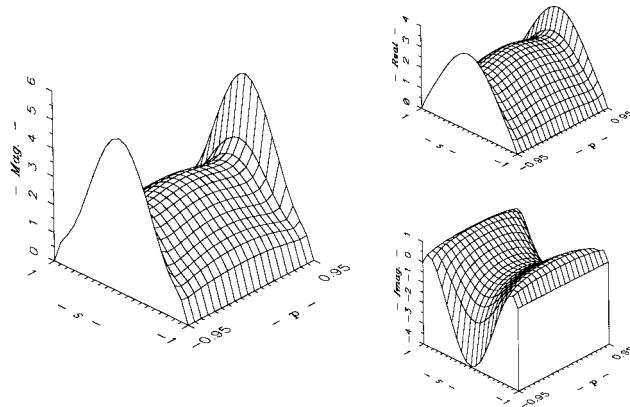


Fig. 5. Benchmark solution ( $n = 8$ ) for the  $s$ -current component over the scatterer. (a) Magnitude. (b) Real part. (c) Imaginary part.

with magnetic field intensity of incident plane wave) over the scatterer. Since the  $p$ -current component is infinite along edges  $s = \pm 1$  this component is shown only for  $-0.95 \leq s \leq 0.95$ . Since the  $s$ -current component is infinite along edges  $p = \pm 1$ , this component is shown only for  $-0.95 \leq p \leq 0.95$ .

## V. COMPARISON OF ROOFTOP AND POLYNOMIAL BASIS FUNCTIONS

The solution adopted as a benchmark is applied for the comparison of polynomial entire-domain basis functions (given by (8) and (9), but with symmetry not taken into account) and rooftop basis functions. All results (except the benchmark solution) are obtained by the program WIPL at IBM AT-486 on 33 MHz [14].

In the case when rooftop basis functions are used, the scatterer is uniformly divided into patches. (The patches are squares of equal size.) The number of patches along one scatterer side is designated by  $n$ . It is easy to show that the number of unknowns  $N$  corresponding to the order of polyno-

TABLE III

THE NUMBER OF UNKNOWN  $N$  CORRESPONDING TO THE ORDER OF POLYNOMIAL APPROXIMATION  $n$ . (THE SAME RELATION EXISTS BETWEEN THE NUMBER OF ROOFTOP BASIS FUNCTIONS AND THE NUMBER OF CORRESPONDING PATCHES ALONG THE SCATTERER SIDE)

$n$	2	3	4	5	6	7	8	9	10	11	12	13	14	15	16
$N$	4	12	24	40	60	84	112	144	180	220	264	312	364	420	480

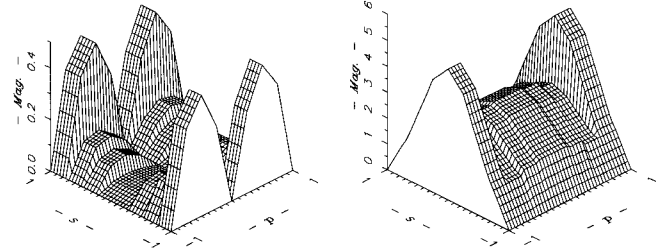


Fig. 6. Rooftop solution ( $n = 8$ ) for magnitude of (a)  $p$ -current component and (b)  $s$ -current component over the scatterer.

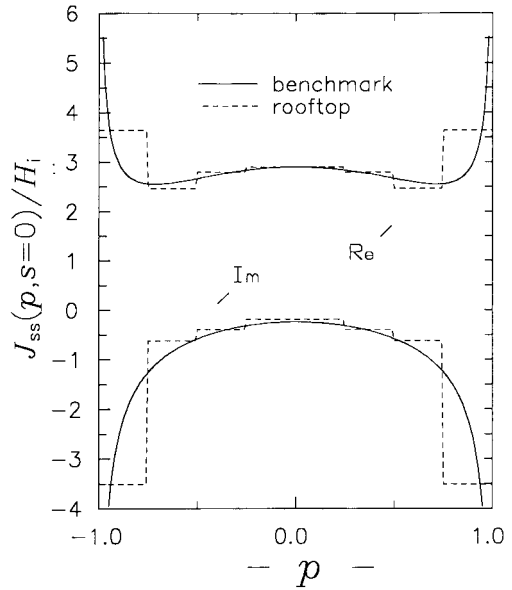


Fig. 7. Rooftop and benchmark solutions ( $n = 8$ ) for  $s$ -current component along the  $p$ -axis (real and imaginary parts).

mial approximation  $n$  is equal to the number of rooftop basis functions if the number of patches along one scatterer side is also  $n$ . The relation between  $N$  and  $n$  is given in Table III.

Fig. 6 shows magnitude of  $p$  and  $s$ -current component over the scatterer, obtained with rooftop basis functions for  $n = 8$  ( $N = 112$ ). Fig. 7 shows magnitude of  $s$ -component along  $p$ -coordinate axis obtained with rooftop basis functions for  $n = 8$  ( $N = 112$ ). When these graphs are compared with Figs. 2, 4, and 5 it can be concluded that rooftop basis functions cannot easily follow fast changes of currents, which is particularly pronounced in the transversal direction (i.e., direction normal to the current flow). This can be explained by two facts. First, current changes in the transversal direction are much more pronounced than current changes in the longitudinal direction. Second, piecewise constant approximation used in the transversal direction is much poorer than piecewise linear approximation used in longitudinal direction.

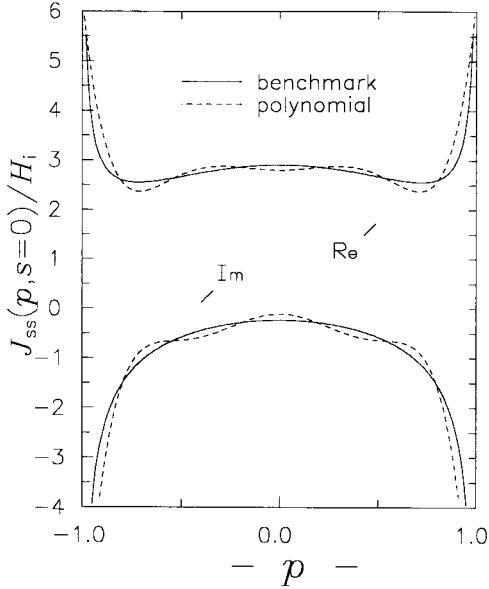


Fig. 8. Polynomial and benchmark solutions ( $n = 8$ ) for  $s$ -current component along the  $p$ -axis (real and imaginary parts).

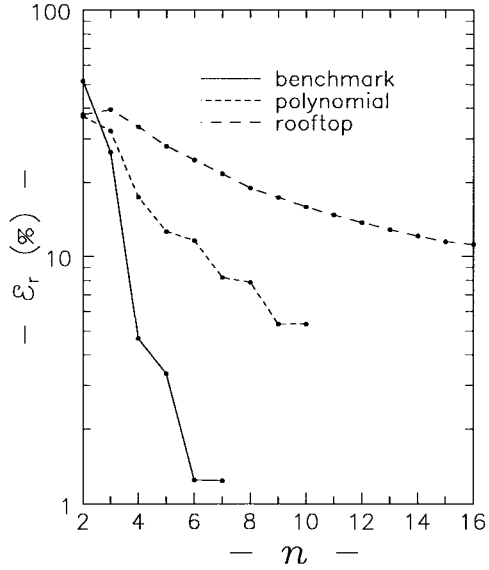


Fig. 9. Relative error of approximation for  $s$ -current component versus the order of approximation. The relative error is evaluated for benchmark solutions ( $n < 8$ ), polynomial solutions, and rooftop solutions.

Fig. 8 shows magnitude of  $s$ -component along  $p$ -coordinate axis, obtained with polynomial basis functions for  $n = 8$  ( $N = 112$ ). Corresponding three-dimensional graphs for current distribution are omitted because they are very similar to the graphs shown in Figs. 4 and 5. Having this in mind and comparing Fig. 8 with Fig. 2, it can be concluded that polynomial basis functions enable very accurate approximation of the current, except very close to the scatterer edges. Besides that, it can be concluded that polynomial basis functions enable more efficient approximation than rooftop basis functions. In order to obtain quantitative measure of efficiency of these functions, let us apply error metric given by (2).

Fig. 9 shows relative error of approximations for  $s$ -current component versus the order of approximation  $n$ . The relative

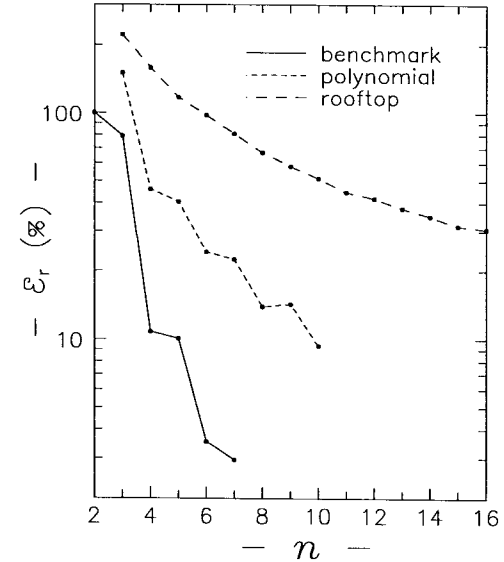


Fig. 10. Relative error of approximation for  $p$ -current component versus the order of approximation. The relative error is evaluated for benchmark solutions ( $n < 8$ ), polynomial solution, and rooftop solution.

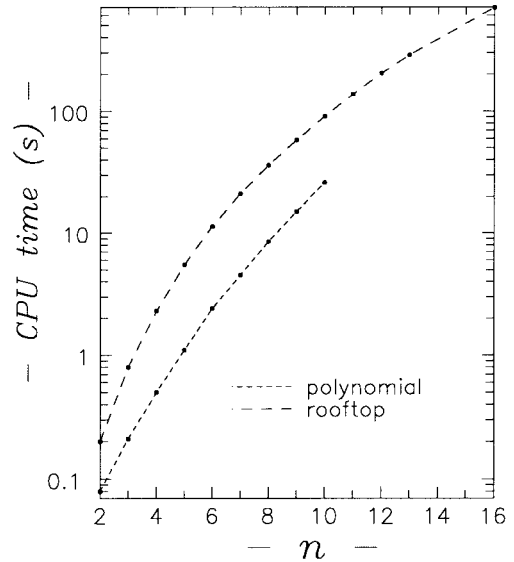


Fig. 11. CPU time used for polynomial and rooftop analysis versus the order of approximation.

error is evaluated for benchmark solutions (for  $n < 8$ ), polynomial solutions, and rooftop solutions. Fig. 10 shows the same as Fig. 9 but for  $p$ -current component. (Since the  $s$ -current component is much greater than the  $p$ -current component, relative error of approximation for the total current is almost the same as the relative error of approximation for  $s$ -current component.) It can be seen from these figures that for the same accuracy required the rooftop solution needs few times greater order of approximation than the polynomial solution and the polynomial solution needs few times greater order of approximation than the benchmark solution.

Fig. 11 shows central processing unit (CPU) time used for analysis versus the order of approximation  $n$ . Only curves for polynomial and rooftop solutions are given. It is seen that for the same order of approximation rooftop

TABLE IV

ORDER OF APPROXIMATION  $n$ , NUMBER OF UNKNOWNNS  $N$ , AND CPU TIME USED IN THE ANALYSIS BASED ON POLYNOMIAL AND ROOFTOP BASIS FUNCTIONS. REQUIRED RELATIVE ERROR FOR  $s$ -CURRENT COMPONENT IS LESS THAN  $E = 20\%$  AND  $E = 10\%$

	$E = 20\%$			$E = 10\%$		
	$n$	$N$	CPU	$n$	$N$	CPU
rooftop	8	112	9	17	564	954
polynomial	4	24	0.5	7	84	4.4

TABLE V

ORDER OF APPROXIMATION  $n$ , NUMBER OF UNKNOWNNS  $N$  AND CPU TIME USED IN THE ANALYSIS, BASED ON POLYNOMIAL AND ROOFTOP BASIS FUNCTIONS. REQUIRED RELATIVE ERROR FOR  $p$ -CURRENT COMPONENT IS LESS THAN  $E = 50\%$  AND  $E = 30\%$

	$E = 50\%$			$E = 30\%$		
	$n$	$N$	CPU	$n$	$N$	CPU
rooftop	11	220	104	16	480	700
polynomial	4	24	0.5	6	60	1.2

solution needs much more CPU time than the polynomial solution.

Starting from Figs. 9, 10, and 11 and Table III it is possible to determine the number of unknowns and CPU time of analysis needed for accuracy required. Table IV gives order of approximation  $n$ , number of unknowns  $N$ , and CPU time used in the analysis if required relative error for  $s$ -current component is less than  $E = 20\%$  and  $E = 10\%$ . (Only data for polynomial and rooftop solutions are given.) Table V gives the same data as Table IV, but for  $p$ -current component and the required relative error is less than  $E = 50\%$  and  $E = 30\%$ . It is seen from the table that rooftop solution needs five to ten more unknowns and 20–500 more CPU time than the polynomial solution for the same accuracy required.

## VI. CONCLUSION

The accurate solution of current distribution over square scatterer is found in the form of a double series of basis functions automatically satisfying the continuity equation at plate edges and including the edge effect. It is shown that such a solution converges very fast with increasing the order of approximation. The solution obtained for the order of approximation  $n = 8$  is adopted as a benchmark. Namely, this solution is enough accurate and consists of not too many basis functions. (The total number of basis functions used for both current components is 28.)

The solution adopted as a benchmark is used for comparison of rooftop basis functions and polynomial entire-domain basis functions. The numerical results show that in the case of square scatterer the polynomial approximation is much more efficient than that by rooftop basis functions. Particularly, the following cases are considered: relative error for  $s$ -current component should be less than  $E = 20\%$  and  $E = 10\%$  and relative error for  $p$ -current component should be less than  $E = 50\%$  and  $E = 30\%$ . In these cases, the rooftop solution needs five to ten more unknowns and 20–500 more CPU time than the polynomial solution. The numerical results also show that in the case considered the efficiency of the analysis performed

by polynomial entire-domain basis functions can be further significantly improved by inclusion the edge conditions.

Finally, it should be noted that an overall validation of numerical methods for electromagnetic modeling of plate structures cannot be based on one benchmark solution. Hence, in the process of such validation, the benchmark solution given in this paper should be combined with other benchmarks that can be found in the open literature.

## REFERENCES

- [1] R. F. Harrington, *Field Computation by Moment Methods*. New York: McMillan, 1968.
- [2] J. R. Mautz and R. F. Harrington, "Radiation and scattering from bodies of revolution," *J. Appl. Sci. Res.*, vol. 20, pp. 405–413, 1969.
- [3] D. L. Knepp and J. Goldhirsh, "Numerical analysis of electromagnetic radiation properties of smooth conducting bodies of arbitrary shape," *IEEE Trans. Antennas Propagat.*, vol. AP-20, pp. 383–388, May 1972.
- [4] N. C. Albertsen, J. E. Hansen, and N. E. Jensen, "Computation of radiation from wire antennas on conducting bodies," *IEEE Trans. Antennas Propagat.*, vol. AP-22, pp. 200–206, Mar. 1974.
- [5] N. N. Wang, J. H. Richmond, and M. C. Gilreath, "Sinusoidal reaction formulation for radiation and scattering from conducting surfaces," *IEEE Trans. Antennas Propagat.*, vol. AP-23, pp. 376–382, May 1975.
- [6] E. H. Newman and D. M. Pozar, "Electromagnetic modeling of composite wire and surface geometries," *IEEE Trans. Antennas Propagat.*, vol. AP-26, pp. 784–789, Nov. 1978.
- [7] A. W. Glisson and D. R. Wilton, "Simple and efficient numerical methods for problems of electromagnetic radiation and scattering from surfaces," *IEEE Trans. Antennas Propagat.*, vol. AP-28, pp. 593–603, Sept. 1980.
- [8] J. F. Shaeffer and L. N. Medgyesi-Mitschang, "Radiation from wire antenna attached to bodies of revolution: The junction problem," *IEEE Trans. Antennas Propagat.*, vol. AP-29, pp. 479–487, May 1981.
- [9] S. M. Rao, D. R. Wilton, and A. W. Glisson, "Electromagnetic scattering by surfaces of arbitrary shape," *IEEE Trans. Antennas Propagat.*, vol. AP-30, pp. 409–418, May 1982.
- [10] J. M. Bornholdt and L. N. Medgyesi-Mitschang, "Mixed-domain Galerkin expansions in scattering problems," *IEEE Trans. Antennas Propagat.*, vol. 36, pp. 216–227, Feb. 1988.
- [11] B. M. Kolundžija, "Electromagnetic modeling of wire-to-plate structures," D.Sc. dissertation, Univ. Belgrade, Yugoslavia, 1990 (in Serbian).
- [12] ———, "General entire-domain Galerkin method for electromagnetic modeling of composite wire and plate structures," in *Proc. 20th Eur. Microwave Conf.*, Budapest, Hungary, Sept. 1990, pp. 853–858.
- [13] B. M. Kolundžija and B. D. Popović, "Entire-domain Galerkin method for analysis of generalized wire antennas and scatterers," *Proc. Inst. Elect. Eng.*, vol. 139, pp. 17–24, Feb. 1992.
- [14] B. M. Kolundžija, J. S. Ognjanović, T. K. Sarkar, and R. F. Harrington, *WIPL: Electromagnetic Modeling of Composite Wire and Plate Structures—Software and User's Manual*. Norwood, MA: Artech House, 1995.
- [15] J. Van Bladel, *Electromagnetic Fields*. New York: McGraw-Hill, 1964.
- [16] C. J. Railton, T. Rozzi, and J. Kot, "The efficient calculation of high order shielded microstrip modes for use in discontinuity problems," in *Proc. 16th Eur. Microwave Conf.*, Dublin, Ireland, Sept. 1986, pp. 529–533.



**Branko M. Kolundžija** (M'92) was born in Zenica, Yugoslavia, in 1958. He received the B.Sc., M.Sc., and D.Sc. degrees from the University of Belgrade, Belgrade, Yugoslavia, in 1981, 1986, and 1990, respectively.

In 1981, he joined the School of Electrical Engineering, University of Belgrade, where he is currently an Associate Professor in electromagnetics and antennas and propagation. He is the author or coauthor of nine journal articles, a monograph on analysis of metallic structures, and a software package for electromagnetic modeling of combined wire-to-plate structures. His research interests include numerical problems in electromagnetics, especially those applied to antennas and microwave components.